Published in final edited form as:
Exp Neurol. 2011 January ; 227(1): 149–158. doi:10.1016/j.expneurol.2010.10.010.

Ultrastructural relationship between the AMPA-GluR2 receptor subunit and the mu-opioid receptor in the mouse central nucleus of the amygdala

Marc A. Beckerman and **Michael J. Glass***
Department of Neurology and Neuroscience, Weill Cornell Medical College, NY, NY 10065

Abstract

Activation of GluR2 expressing non-calcium permeable AMPA-type glutamate receptors in the central nucleus of the amygdala (CeA) may play an important role in integrating emotion and memory with goal directed behaviors involved in opioid addiction. The location of non-calcium permeable AMPA receptors within distinct neuronal compartments (i.e. soma, dendrite, or axon) is an important functional feature of these proteins, however, their ultrastructural location and subcellular relationship with mu-opioid receptors (μOR) in the CeA are unknown. Immunocytochemical electron microscopy was used to characterize the ultrastructural distribution of GluR2 and its association with μOR in the mouse CeA. A single labeling analysis of GluR2 distribution employing immunoperoxidase or immunogold markers revealed that this protein was frequently affiliated with intracellular vesicular organelles, as well as the plasma membrane of CeA neuronal profiles. Among all GluR2 labeled neuronal structures, over 85% were dendrites or somata. Unlabeled axon terminals frequently formed asymmetric excitatory-type synaptic junctions with GluR2 labeled dendritic profiles. Dual labeling immunocytochemical analysis showed that GluR2 and μOR were co-localized in neuronal compartments. Among all dual labeled structures, approximately 80% were dendritic. Synaptic inputs to these dual labeled dendrites were frequently from unlabeled axon terminals forming asymmetric excitatory-type synapses. The presence of GluR2 in dendritic profiles receiving asymmetric synapses suggests that activation of the non-calcium permeable AMPA receptor plays a role in the postsynaptic modulation of excitatory signaling involving CeA neuronal circuits that coordinate sensory, affective, and behavioral processes involved in drug addiction. Given the critical role of non-calcium permeable AMPA receptor function in neural and behavioral adaptability, their dendritic association with μOR in CeA dendrites provides a neuronal substrate for opioid-mediated plasticity.

Keywords

Addiction; Glutamate; Opioids; Synaptic Plasticity

*Correspondence to: Dr. Michael J. Glass, Department of Neurology and Neuroscience, 407 E. 61st St., Weill Cornell Medical College, NY, NY 10065. mjg2003@mail.med.cornell.edu.

INTRODUCTION

The central nucleus of the amygdala (CeA) is an important component of neural systems that coordinate sensory and affective processes with memory and goal directed behaviors (Lang and Davis, 2006). The CeA is also emerging as a key neuroanatomical substrate of addiction to psychoactive drugs (Koob and Volkow, 2010) including opioids (Glass, 2010), a phenomenon that critically involves glutamate signaling. The CeA receives diverse information related to sensory experience, emotional state, and memory from glutamatergic inputs originating in the thalamus (Turner and Herkenham, 1991), limbic cortex (Fisk and Wyss 2000,; McDonald, 1998), basolateral nucleus of the amygdala [BLA; (Pitkanen et al. 1997)], and the hippocampal formation (Cullinan et al., 1993; Kishi et al., 2006). Neurons in the CeA integrate these and other signals, particularly from midbrain and brainstem catecholaminergic neurons (Asan, 1998). Through its outputs to areas of the extended amygdala, hypothalamus, and brain stem, the CeA, in turn, plays an important role in modulating autonomic, neuroendocrine, and behavioral processes critical to homeostatic regulation (Knapska et al., 2007; LeDoux, 2000).

Most fast excitatory neurotransmission in the CeA, as in other areas of the central nervous system, is mediated by AMPA-type glutamate receptors (Palmer et al., 2005; Shindou et al., 1993). The AMPA receptors are diverse tetrameric assemblages of various combinations of the four AMPA receptor subunits (GluR1-4) that are encoded by separate genes (Cull-Candy et al., 2006). Because of their heterogeneous subunit composition and post-transcriptional modifications, AMPA receptors express highly diverse biophysical features including channel opening properties and Ca^{2+} permeability (Cull-Candy et al., 2006). Receptors expressing the GluR2 subunit are particularly noteworthy because of their Ca^{2+} impermeability. In addition, experience-dependent trafficking of non-calcium permeable AMPA receptors between intracellular and plasma membrane locations is an established component of neural plasticity (Bassani et al., 2009) and an emerging feature of addictive behaviors including cue-induced relapse to heroin seeking (Van den Oever et al., 2008).

The expression of non-calcium permeable AMPA receptors in neuronal compartments (i.e. soma, dendrite, or axon) is an important functional property of these proteins (Petralia et al., 1997). Within neurons, it has been reported that non-calcium permeable AMPA receptors may be limited to the soma (Lerma et al., 1994), however, other reports indicate a wider pattern of expression, including somata and dendrites (Spruston et al., 1995). When present in dendrites, GluR2 has been shown to have diverse relationships to synaptic inputs, including expression at plasmalemmal sites receiving asymmetric excitatory-type synaptic specializations, as well as extrasynaptic areas of the plasma membrane adjacent to symmetric synapses (He et al., 1998). In addition to their presence in somata and dendrites, non-calcium permeable AMPA receptors may also be expressed in presynaptic structures in certain neural areas (Fabian-Fine et al., 2000). Based on this evidence, the synaptic organization of non-calcium permeable AMPA receptors may vary by brain region. Both GluR2 mRNA (Sato et al., 1993) and protein (Petralia and Wenthold, 1992) are abundant in the CeA. However, whether non-calcium permeable AMPA receptors are expressed exclusively in CeA cell bodies, or more broadly in somata and dendritic profiles, including those receiving asymmetric excitatory-type synapses is unknown.

Functional GluR2 containing AMPA receptors play an important role in emotional learning and memory (Mead et al., 2006), processes that are implicated in addictive behaviors. The central amygdala may be an important neuroanatomical substrate for AMPA receptor and μ-opioid receptor (μOR) interactions involved in opioid plasticity. The CeA contains intrinsic neurons and axon terminals that contain opioid peptides (Cassell and Gray, 1989; Fallon and Leslie, 1986; Poulin et al., 2006). Moreover, μORs are expressed in the CeA (Mansour et al.,

1995; Mansour et al., 1988; Poulin et al., 2006), where these proteins are present in postsynaptic structures that also express NMDA-type glutamate receptors and receive excitatory-type synapses (Glass et al., 2009). Central amygdala AMPA receptors have been shown to play important roles in opioid dependence, as demonstrated by reports that pharmacological blockade of AMPA receptors in this nucleus inhibits the physical (Taylor et al., 1998) and conditioned aversive (Watanabe et al., 2002) manifestations of opioid withdrawal. Despite the significance of central amygdala glutamate and opioid signaling in behavioral processes linked with opioid plasticity, the synaptic organization of non-calcium permeable AMPA receptors and μ-opioid receptors in the CeA is unknown.

The high spatial resolution provided by electron microscopic immunocytochemistry employing visually distinct gold and peroxidase markers provides a powerful tool to investigate the synaptic organization of distinct receptor systems. This approach was used to characterize the fine structural distribution of GluR2 in the CeA, as well as the ultrastructural relationship between GluR2 and μ-opioid receptors in this brain area. Given the importance of mouse genetic models in neurobiological studies of addiction and other psychiatric syndromes, electron microscopic analyses were performed in the CeA of this species.

METHODS

Subjects

The experimental protocols were carried out in accordance with the National Institutes of Health Guide for the Care and Use of Laboratory Animals and were approved by the Institutional Animal Care and Use Committees at the Weill Cornell Medical College. All efforts were made to minimize the number of animals used and their suffering. Male C57/BL/6 mice weighing 20-25 grams were housed in groups of 2-4 animals per cage and maintained on a 12-hr light/dark cycle (lights out 1800 hours). All mice had unlimited access to water and rodent chow in their home cages.

Tissue preparation and single labeling immunocytochemical procedures

A total of 10 mice were anesthetized with pentobarbital (150 mg/kg, i.p.), and their brains were fixed by aortic arch perfusion sequentially with: (a) 15 ml of normal saline (0.9%) containing 1000 units/ml of heparin, (b) 40 ml of 3.75% acrolein in 2% paraformaldehyde in 0.1 M phosphate buffer (PB, pH 7.4), and (c) 100 ml of 2% paraformaldehyde in PB, all delivered at a flow rate of 100 ml/minute. The brains were removed and post-fixed for 30 minutes in 2% paraformaldehyde in PB. Coronal sections (40 μm) from the forebrain at the level of the CeA, according to the atlas of Hof et al. (2000), were cut with a vibrating microtome. Forebrain sections obtained from five mice were processed for single immunogold, and five for immunoperoxidase labeling of GluR2. Tissue sections were next treated with 1.0% sodium borohydride in PB and washed in PB. To enhance tissue permeability, sections were immersed in a cryoprotectant solution (25% sucrose and 2.5% glycerol in 0.05 M PB) for 15 minutes, followed by freeze-thawing in liquid freon and liquid nitrogen. Sections were next rinsed in 0.1 M Tris-buffered saline (TBS, pH 7.6) and then incubated for 30 minutes in 0.5% bovine serum albumin (BSA) to minimize nonspecific labeling. Tissue sections were incubated in primary rabbit anti-GluR2 antiserum (ABC: 1:400; Gold:1:100) in TBS for 48 hours. Sections were then washed in TBS, and incubated in anti-rabbit IgG conjugated to biotin, rinsed in TBS, and then incubated for 30 minutes in avidinbiotin-peroxidase complex (ABC; 1:100, Vectastain Elite Kit, Vector Laboratories) in TBS. The bound peroxidase was visualized by reaction for 6 minutes in 0.2% solution of 3, 3′-diaminobenzidine (DAB) and 0.003% hydrogen peroxide in TBS. For exclusive immunogold labeling, sections were rinsed in 0.01 M PBS (pH 7.4), and blocked for 10

minutes in 0.8% BSA and 0.1% gelatin in PBS to reduce non-specific binding of gold particles. Sections then were incubated for 2 hours in anti-rabbit IgG conjugated with 1 nm gold particles (1:50, AuroProbeOne, Amersham, Arlington Heights, IL), then rinsed in 0.5% BSA and 0.1% gelatin in PBS, and then PBS. After gold conjugated secondary antisera incubation, sections were incubated for 10 minutes in 2% glutaraldehyde in PBS, and rinsed in PBS. The bound gold particles were enlarged by a 6 minute silver intensification using an IntenSE-M kit (Amersham, Arlington Heights, IL). A few immunolabeled sections were mounted, dehydrated, and coverslipped on glass slides. These sections were examined using a Nikon light microscope. The majority of the labeled sections were processed for electron microscopy.

Dual labeling immunocytochemical procedures

Sections were processed for dual labeling of GluR2 by immunogold and μOR by immunoperoxidase in six mice, and markers were reversed in a subgroup of three mice. Tissue sections were processed for dual labeling immunocytochemistry as previously described (Chan et al., 1990; Leranth and Pickel, 1989). Briefly, sections were incubated for 48 hours in a primary antiserum cocktail including GluR2 (peroxidase: 1:400; gold: 1:100) and μOR (peroxidase:1:400; gold: 1:100). After incubation, sections were rinsed in TBS and prepared first for peroxidase identification. Sections were incubated in anti-rabbit or anti-guinea pig IgG conjugated to biotin, rinsed in TBS, and then incubated for 30 minutes in avidin-biotin-peroxidase complex (1:100, Vectastain Elite Kit, Vector Laboratories) in TBS. The bound peroxidase was visualized by reaction for 5-6 minutes in a 0.2% solution of 3, 3'-diaminobenzidine and 0.003% hydrogen peroxide in TBS, followed by several washes in TBS. In preparation for immunogold labeling, sections were rinsed in 0.01 M PBS (pH 7.4), and blocked for 10 minutes in 0.8% BSA and 0.1% gelatin in PBS to reduce non-specific binding of gold particles. Sections then were incubated for 2 hours in anti-guinea pig or anti-rabbit IgG conjugated with 1 nm gold particles (1:50, AuroProbeOne, Amersham, Arlington Heights, IL), then rinsed in 0.5% BSA and 0.1% gelatin in PBS, and then PBS. In order to investigate possible cross-reactivity, tissue was processed with omission of one or the other primary antisera followed by incubation with the secondary antisera corresponding to the alternate species. Following gold conjugated antisera incubation, sections were then incubated for 10 minutes in 2% glutaraldehyde in PBS, and rinsed in PBS. The bound gold particles were enlarged by a 6 minute silver intensification using an IntenSE-M kit (Amersham, Arlington Heights, IL). The tissue was then postfixed in 2% osmium tetroxide in PB for one hour, and dehydrated in a series of alcohols, through propylene oxide, and flat embedded in EM BED 812 (EMS, Fort Washington, PA) between 2 sheets of Aclar plastic.

Antisera

Brain sections containing the amygdala were processed for exclusive GluR2 labeling, or dual labeling with μOR using affinity purified polyclonal rabbit and guinea pig antipeptide antisera, respectively (Millipore, Billerica, MA). The glutamate receptor subunit antiserum recognizes amino acids 827-842 of rat GluR2. This antibody has been characterized in transfected cells and Western blots of rat brain (Manufacturer's data). The μOR antiserum was raised against amino acids 384-398 of the cloned rat μOR. Immunolabeling of this receptor is abolished by preadsorption with the antigenic peptide (Drake and Milner, 2002), and significantly attenuated in mice with a knockout of either exon 1, 2/3, or 11 of the μOR gene, respectively (Jaferi and Pickel, 2009).

Electron Microscopy

Ultrathin sections (60-80 nm) from the surface of flat-embedded sections containing the CeA (Figure 1) were cut with a diamond knife using an ultramicrotome (Ultratome, NOVA, LKB, Bromma, Sweden), and sections were collected on grids. Electron microscopic images

of this tissue were obtained using a digital camera (Advanced Microscopy Techniques, Danvers, MA) interfaced with a transmission electron microscope (Technai 12 BioTwin, FEI, Hillsboro, OR). The specific fields selected for electron microscopic analysis were randomly chosen from each thin-sectioned tissue sample, however most of these areas showed labeling for either GluR2 or μOR. Sampled fields were captured as digital images using the AMT Advantage HR/HR-B CCD Camera System (AMT, Danvers, MA). For preparation of figures, images were adjusted for contrast and brightness using Photoshop CS4 software, and imported into PowerPoint to add lettering.

Ultrastructural analysis

From the CeA of each animal, three grid squares from 2 ultrathin sections were selected for analysis. In order to control for potential labeling artifacts due to penetration of cytological reagents, sampling was performed at the tissue surface as determined by proximity to the epon-tissue interface. This was achieved by collecting electron micrographs exclusively in the transition zone where one edge of the sampling area was in contact with epon in a field of at least three grid squares. Digital images were captured and analyzed to determine the number of single and dual labeled neuronal and glial profiles. The classification of labeled dendrites was based upon descriptions by Peters et. al. (1991). Dendrites were identified by the presence of postsynaptic densities, as well as ribosome's and both rough and smooth endoplasmic reticula. However, profiles were also considered dendritic whenever postsynaptic densities were observed, independent of endoplasmic reticulum. Somata were distinguished by the presence of a nucleus. Axon terminals were identified by size (at least 0.2 μm diameter) and the presence of synaptic vesicles. Astrocytes were identified by their irregular shape, the presence of filamentous membranes apposing dendrites or axons, or the presence of gap junctions. Synapses were defined as either symmetric or asymmetric, according to the presence of either thin or thick postsynaptic specializations, respectively. Appositions were distinguished by closely spaced plasma membranes that lacked recognizable specializations, or interposing astrocytic processes. Structures containing electron dense granular precipitate darker than that seen in similar processes in the neuropil were considered as containing immunoperoxidase labeling. At least one gold particle per small profile, or two gold particles for larger profiles were considered as evidence of positive immunogold labeling, provided that comparable areas of epon, or neuropil containing myelin or other structures not expressing NR1 or μOR, were devoid of gold-silver deposits (Hara and Pickel, 2008). Under similar conditions of low background, it has been shown that 1-2 gold particles in small profiles, such as dendritic spines, is equivalent to four or more in dendritic profiles with a larger surface area (Wang et al., 2003). Data were analyzed by unpaired t-tests or Analysis of Variance where applicable. Differences in means were analyzed by Fisher's Protected Least Significant Difference.

RESULTS

Visualization of GluR2 labeling in neuronal profiles in the mouse CeA

By light microscopy, GluR2 immunoreactivity was present throughout the CeA (Figure 1), where granular GluR2 immunoreactivity was diffusely distributed throughout the cytoplasm of cell bodies. By electron microscopy, GluR2 labeling was seen in neuronal somata that contained ovoid or irregularly shaped nuclei, Golgi Complexes, numerous vesicular organelles, as well as smooth and rough endoplasmic reticula (Figures 2A-B). Labeling for GluR2 in cell bodies was typically associated with intracellular structures, including the outer membranes of tubulovesicular organelles and Golgi (Figure 2A). Immunoreactivity for GluR2 was occasionally present near the plasma membrane of somata (Figure 2B). Cell bodies were typically apposed by unlabeled dendritic and glial profiles, as well as axons and axon terminals with or without forming synaptic specializations.

Dendritic profiles frequently exhibited GluR2 labeling. Labeled dendritic structures included large, proximal dendritic profiles that contained endoplasmic reticula, mitochondria, as well as small tubulovesicular organelles (Figures 3A-B). In large dendritic profiles, immunoreactivity for GluR2 was typically associated with intracellular vesicular organelles (Figure 3A), and was also seen to a lesser extent on the non-synaptic surface membrane (Figure 3B). Labeled large dendritic profiles were frequently apposed by unlabeled dendritic and glial processes, as well as axon terminals, some of which formed symmetric or asymmetric-type synaptic junctions. Immunoreactivity for GluR2 was also present in medium-size and small distal dendritic profiles (Figures 4A-C). These structures contained mitochondria and small tubulovesicular or ovoid organelles and were contacted by axons and axon terminals that were typically devoid of GluR2 labeling. Immunoreactivity for GluR2 was frequently associated with tubulovesicular structures and the plasma membrane (Figure 4A). Spiny appendages often protruded from GluR2 labeled dendritic shafts, where labeling was observed in the spine neck (Figure 4B) and spine head (Figure 4C) regions. In addition to the extrasynaptic plasmalemma, GluR2 immunoreactivity was also associated with the plasma membrane directly apposed to unlabeled axon terminals (Figure 5A), where labeling was observed in the postsynaptic density of asymmetric excitatory-type synaptic specializations (Figure 5B), particularly when the glutamate receptor subunit was labeled with the immunoperoxidase method.

Immunolabeling for GluR2 was also present at low levels in presynaptic structures (not shown). These included small unmyelinated axons and axon terminals. There was little appreciable evidence of glial labeling.

Quantification of electron microscopic GluR2 labeling in neuronal profiles in the mouse CeA

By electron microscopy, a 22,050 μm^2 area of the CeA was sampled in separate forebrain sections processed for single immunoperoxidase or immunogold labeling of GluR2. A total of 1,316 GluR2 containing profiles were counted, 430 of which were labeled with immunogold, 886 with immunoperoxidase. Although GluR2 was found in diverse neuronal compartments, dendritic profiles were most common (Figure 6; Table 1). There were significantly more GluR2 labeled dendritic profiles as compared to somata (Gold: $t=10.6$, $p<.0005$; Peroxidase: $t=13.2$, $p<.0005$) and axons (Gold: $t=16.6$, $p<.0005$; Peroxidase: $t=11.5$, $p<.0005$). These patterns were independent of secondary antisera labeling conditions. As shown in Figure 6, the number of GluR2 labeled somata [$F(1,8)= 1.6$, $p>.23$], dendrites [$F(1,8)= 2.2$, $p>.17$], or axons [$F(1,8)=1.7$, $p>.22$] did not significantly differ when calculated as a percentage of all labeled profiles when labeled with either the immunogold or immunoperoxidase markers.

In order to determine the relative subcellular distribution of GluR2 in dendritic profiles, immunogold particles were categorized into distinct compartments, including cytoplasmic round or tubulovesicular organelles, as well as the surface membrane. Of all GluR2 immunogold particles, 75 2% were associated with cytosolic organelles, 25 3% were directly in contact with the plasmalemma. There were significantly more gold particles in contact with intracellular organelles compared with the plasma membrane ($t=8.5$, $p<.005$).

A total of 336 contacts between axon terminals and GluR2 labeled dendritic profiles were counted. Contacts were defined as non-synaptic appositions, in addition to symmetric, or asymmetric-type synapses. There were no significant differences in the percentage of appositions ($p>.2$), as well as symmetric ($p>.15$) or asymmetric synapses ($p>.6$) when GluR2 was labeled by immunogold or peroxidase markers, so data from the two labeling conditions were combined to determine the relative percentage of contact-types involving axon terminals and GluR2 labeled dendrites. Approximately 61±2% of contacts were

appositions, while 9±3% were symmetric synapses and 30±2% were asymmetric synaptic specializations. There were significantly more asymmetric synapses compared to symmetric synapses ($t=4.7$, $p<.005$).

Electron microscopic visualization of GluR2 and μOR labeling in the mouse CeA

Electron microscopic analysis of the distribution of GluR2 and μOR in the CeA revealed diverse populations of labeled neuronal profiles. These included single GluR2 or μOR labeled somata and dendritic structures, as well as axons and axon terminals. The ultrastructural distribution of μOR in CeA neurons was comparable to that described in previous publications (Glass et al., 2009; Jaferi and Pickel, 2009). In addition there were numerous examples of neural processes, principally somata and dendrites, co-expressing GluR2 and μOR.

Neuronal somata co-labeled for GluR2 and μOR were similar to those exclusively labeled for the glutamate receptor subunit. These cell bodies typically contained large nuclei, as well as multiple mitochondria and vesicular organelles (Figure 7). In these dually labeled reticula, and small round vesicular organelles. Although individual intracellular organelles osmata, immunoreactivity for either GluR2 or μOR was associated with GCs, endoplasmi reticula, and small round vesicular organelles. Although individual intracellular organelles frequently contained labeling exclusively for only one of the proteins, there were also examples of overlapping GluR2 and μOR in common Golgi or endoplasmic reticula (Figure 7, insets).

Both GluR2 and μOR were frequently present in dendritic profiles. These included large proximal dendrites, where GluR2 and μOR were typically associated with intracellular membranous organelles and, to a lesser extent, the plasma membrane (not shown). The glutamate receptor subunit and the opioid receptor were also frequently present in common small distal dendrites (Figures 8A-B). These GluR2 labeled dendritic structures were contacted by unlabeled glial profiles, as well as axon terminals, which formed non-synaptic appositions in addition to synaptic specializations. In these profiles, immunolabeling for GluR2 and μOR were associated with separate, closely apposed, or common intracellular organelles (Figures 9A-B) as well as areas of the plasmalemma (Figures 8A-B). Although GluR2, and, to a greater extent μOR, were seen in presynaptic structures, there were few instances of co-labeling in axons or axon terminals, and no appreciable glial co-labeling.

Electron microscopic quantification of GluR2 and μOR co-expression in neuronal profiles in the mouse CeA

In tissue processed for dual labeling of GluR2 by immunogold and μOR by peroxidase, as well as with the markers reversed, a total of 1,614 labeled profiles were counted in a 17,325 μm^2 area of the CeA. A total of 585 labeled profiles were exclusively labeled for GluR2, 801 were singly labeled for μOR, and the remaining 206 profiles were dually labeled. The number of somata, dendrites, and axons labeled exclusively for GluR2 or μOR, as well as expressing labeling for both are presented in Table 2. There were significantly more dual labeled dendritic profiles as compared to somata (Figure 10) when GluR2 was labeled with immunogold and μOR by immunoperoxidase ($t=5.3$, $p<.005$) and when the markers were reversed ($t=4.8$, $p<.05$). Similarly, there were significantly more dual labeled dendrites compared to axons when GluR2 was labeled with gold and μOR by peroxidase ($t=9.8$, $p<.0005$) and when the markers were reversed ($t=10.9$, $p<.01$). As shown in Figure 10, there were no significant differences in the relative proportion of dual labeled somata [$F(1,7)= .6$, $p>.4$], dendrites [$F(1,7)= .6$, $p>.4$], or axons [$F(1,7)=.03$, $p>.8$] calculated as a percentage of all dual labeled profiles when GluR2 was labeled with immunogold and μOR by immunoperoxidase and when the markers were reversed.

A total of 99 contacts between axon terminals and dual labeled dendritic profiles were counted. There were no significant differences in the percentages of appositions ($p>.65$), as well as symmetric ($p>.6$) or asymmetric synapses ($p>.15$) in either secondary labeling combination. Therefore all contacts involving dual labeled dendrites were combined to determine the relative number of contact-types involving these structures. Approximately 66±4% were appositions, while 5±2% were symmetric and 29±4% asymmetric-type synaptic junctions. There were significantly more asymmetric synapses compared to symmetric synapses ($t=4.9$, $p<.005$).

DISCUSSION

This is the first characterization of the fine structural distribution of GluR2, and its relationship to the mu-opioid receptor in neuronal profiles from the mouse central nucleus of the amygdala. The present results demonstrate that GluR2 is mainly present in dendritic profiles, including those receiving asymmetric excitatory-type synapses. Moreover, many GluR2 labeled postsynaptic structures also exhibit immunoreactivity for μOR. These results provide ultrastructural evidence that non-calcium permeable AMPA receptors and mu-opioid receptors play a role in the modulation of excitatory signaling in dendritic compartments of CeA neurons.

GluR2 is expressed in dendrites and somata of CeA neurons

Immunocytochemical electron microscopic analysis revealed that GluR2 was present in neuronal cell bodies, where discrete punctate GluR2 labeling was associated with intracellular organelles involved in protein synthesis, packaging and transport. These intracellular structures included endoplasmic reticula, where AMPA receptor subunits have been shown to be assembled into tetrameric complexes (Greger and Esteban, 2007). In addition, GluR2 was also affiliated with Golgi Complexes, as well as membranes of small round vesicular organelles, and to a lesser degree, near the plasmalemma. Dendritic processes were frequently labeled with GluR2. These included large proximal dendritic profiles, but also medium and small distal dendritic structures. Labeling for GluR2 was also present in dendritic spines, including both the neck and head of spiny appendages. When axon terminals formed identifiable synapses with GluR2 labeled dendritic profiles these were most commonly asymmetric-type junctions (Peters et al., 1991). These results are consistent with a model of non-calcium permeable AMPA receptors as regulating excitatory inputs in dendrites (He et al., 1999). An analysis of gold particle distribution in dendritic processes showed that GluR2 was associated with two major subcellular compartments. Firstly, this protein was present in small round or tubulovesicular organelles located in the interior of the dendritic shaft or immediately beneath the surrounding surface membrane, including areas in close proximity to the neck of spiny appendages. Secondly, GluR2 was also associated with the plasma membrane, including extrasynaptic and perisynaptic sites. The ratio of intracellular to surface GluR2 levels found in CeA neurons is consistent with prior reports (Palmer et al., 2005).

In sum, GluR2 appears to be actively synthesized, processed, and transported within somata and trafficked throughout dendritic processes of CeA neurons under basal conditions. The presence of GluR2 on functional surface compartments of dendritic and spiny processes receiving excitatory-type contacts indicates that non-calcium permeable glutamate receptors are positioned for the mediation of fast excitatory signaling by glutamate released from axon terminals arising from cerebral cortical, thalamic, hippocampal, and amygdala brain areas in response to novel or learned environmental challenges (Glass, 2010). In addition, there appear to be ample reserve pools of these proteins, both in endosomal compartments and on the extrasynaptic surface membrane. These may serve as a reservoir of receptor capable of

being mobilized by shifting demands of synaptic activity, a phenomenon that may play a critical role in early stages of neural plasticity (Bassani et al., 2009).

GluR2 and μOR are co-expressed in dendrites and somata of CeA neurons

Dual labeling electron microscopic immunocytochemical analysis revealed a diversity of neuronal structures in the CeA. These included dendrites, axons, and somata exclusively labeled for GluR2 or μOR. There were also numerous examples of neuronal profiles in the CeA that were dually labeled for the glutamate and opioid receptors. Cell bodies co-labeled for GluR2 and μOR were similar in fine structural detail to those exclusively labeled for GluR2, as described above. In dually labeled somata, immunoreactivity for either GluR2 or μOR was associated with Golgi, endoplasmic reticula, and small round vesicular organelles. Immunoreactivity for both proteins was found to label separate as well as common GCs and endomembranes.

Both GluR2 and μOR were frequently present in common dendrites. Dendritic profiles that expressed labeling for both proteins were heterogeneous in size. These included large proximal dendrites, where GluR2 and μOR were each typically associated with intracellular membranous organelles and the plasma membrane. The glutamate receptor subunit and the opioid receptor were also frequently present in common small distal dendrites and dendritic spines. In these dual labeled structures, GluR2 and μOR were associated with intracellular vesicular organelles, frequently near the plasma membrane, including beneath spine necks. These co-labeled processes were contacted by unlabeled axon terminals forming non-synaptic appositions and asymmetric excitatory synapses. The presence of GluR2 and μOR in common dendritic profiles was similar to the frequent co-localization of μOR and NMDA receptors in postsynaptic structures in the CeA (Glass et al., 2009), indicating that non-calcium permeable AMPA receptors are expressed with the NMDA receptors in at least some opioid responsive CeA neurons.

Not only were GluR2 and μOR co-expressed in dendritic profiles, they were also frequently associated with common intracellular organelles, as well as adjacent areas of the surface membrane. Similarly, in cell bodies GluR2 and μOR labeled common Golgi Complexes and endoplasmic reticula. This close spatial relationship raises the possibility that these proteins can form larger macromolecular complexes, through direct heterodimerization or by indirect linkage. Although heterodimerization of ionotropic and G-protein coupled receptors (GPCRs) has been reported (Bouvier, 2001), currently, there does not appear to be any evidence for the existence of non-calcium permeable AMPA-mu-opioid receptor complexes. Alternatively, indirect interactions between AMPA receptors and μOR involving one or more shared intermediate scaffolding or adaptor protein is another possibility. In addition to their interactions with GPCRs there are a number of GPCR-interacting proteins that also link AMPA receptors with the cytoskeleton to form larger signaling complexes (Bockaert et al., 2010). Moreover, inhibiting the activity of some of these GPCR-interacting proteins has been shown to influence μOR agonist-induced signal transduction (Garzon et al., 2004). The possibility that non-calcium permeable AMPA receptors and μ-opioid receptors form macromolecular protein complexes awaits direct confirmation.

GluR2 expressing AMPA receptors and μORs: Functional implications

Behavioral pharmacological evidence indicates that functional AMPA receptors play an important role in opioid addictive behaviors. For example, AMPA receptor antagonists have been shown to inhibit physical symptoms of opioid antagonist precipitated morphine (Rasmussen and Vandergriff, 2003) and heroin (Klein et al., 2008) withdrawal, as well as acute opioid withdrawal-induced place aversion (Kawasaki et al., 2005). In addition, it has been reported that blockade of AMPA receptors attenuates the expression of morphine

conditioned place preference (Layer et al., 1993; Tzschentke and Schmidt, 1997) and the development of behavioral sensitization to morphine (Carlezon et al., 1999). Among the various AMPA receptor combinations, those expressing the GluR2 subunit are the most abundant, determine calcium permeability, and have been significantly implicated in neural plasticity (Bassani et al., 2009). Chronic opioid exposure, as well as opioid withdrawal have been shown to influence the expression of GluR2 in various brain areas (Sepehrizadeh et al., 2008; Zhong et al., 2006). Given the significant role of experience-dependent modulation of non-calcium permeable AMPA receptor function in cellular and *in vivo* models of learning and information storage (Sacktor, 2008), phenomena that parallel opioid addictive processes (Van den Oever et al., 2008), interactions between GluR2 expressing AMPA receptors and μORs in dendrites of CeA neurons may represent a fine structural neuronal substrate subserving intracellular events involved in emotional learning and memory linked with opioid use (Migues et al., 2010). In addition, the potential coupling of non-calcium permeable AMPA receptors and mu-opioid receptors is also relevant given the emergence of protein-protein interaction inhibitors as potential pharmacotherapeutic agents (Blazer and Neubig, 2009).

Acknowledgments

Supported by DA-027128 and DA-024030

REFERENCES

Asan E. The catecholaminergic innervation of the rat amygdala. Advances in Anat., Embryol., and Cell Biol 1998;142:1–118. [PubMed: 9586282]

Bassani S, Valnegri P, Beretta F, Passafaro M. The GLUR2 subunit of AMPA receptors: synaptic role. Neurosci 2009;158:55–61.

Blazer LL, Neubig RR. Small molecule protein-protein interaction inhibitors as CNS therapeutic agents: current progress and future hurdles. Neuropsychopharmacol 2009;34:126–41.

Bockaert J, Perroy J, Becamel C, Marin P, Fagni L. GPCR interacting proteins (GIPs) in the nervous system: Roles in physiology and pathologies. Annu. Rev. Pharmacol. Toxicol 2010;50:89–109. [PubMed: 20055699]

Bouvier M. Oligomerization of G-protein-coupled transmitter receptors. Nature Rev. Neurosci 2001;2:274–86. [PubMed: 11283750]

Carlezon WAJ, Rasmussen K, Nestler EJ. AMPA antagonist LY293558 blocks the development, without blocking the expression, of behavioral sensitization to morphine. Synapse 1999;31:256–62. [PubMed: 10051106]

Cassell MD, Gray TS. Morphology of peptide-immunoreactive neurons in the rat central nucleus of the amygdala. J. of Comp. Neurol 1989;281:320–33. [PubMed: 2468696]

Chan J, Aoki C, Pickel VM. Optimization of differential immunogold-silver and peroxidase labeling with maintenance of ultrastructure in brain sections before plastic embedding. J. Neurosci. Methods 1990;33:113–127. [PubMed: 1977960]

Cull-Candy S, Kelly L, Farrant M. Regulation of Ca2+-permeable AMPA receptors: synaptic plasticity and beyond. Curr. Opin. Neurobiol 2006;16:288–97. [PubMed: 16713244]

Cullinan WE, Herman JP, Watson SJ. Ventral subicular interaction with the hypothalamic paraventricular nucleus: evidence for a relay in the bed nucleus of the stria terminalis. J. Comp. Neurol 1993;332:1–20. [PubMed: 7685778]

Drake CT, Milner TA. Mu opioid receptors are in discrete hippocampal interneuron subpopulations. Hippocampus 2002;12:119–36. [PubMed: 12000113]

Fabian-Fine R, Volknandt W, Fine A, Stewart MG. Age-dependent pre- and postsynaptic distribution of AMPA receptors at synapses in CA3 stratum radiatum of hippocampal slice cultures compared with intact brain. Eur. J. Neurosci 2000;12:3687–700. [PubMed: 11029638]

Fallon JH, Leslie FM. Distribution of dynorphin and enkephalin peptides in the rat brain. J. Comp. Neurol 1986;249:293–336. [PubMed: 2874159]

Fisk GD, Wyss JM. Descending projections of infralimbic cortex that mediate stimulation-evoked changes in arterial pressure. Brain Res 2000;859:83–95. [PubMed: 10720617]

Garzon J, Rodriguez-Munoz M, Lopez-Fando A, Garcia-Espana A, Sanchez-Blazquez P. RGSZ1 and GAIP regulate mu- but not delta-opioid receptors in mouse CNS: role in tachyphylaxis and acute tolerance. Neuropsychopharmacol 2004;29:1091–104.

Glass MJ. The role of functional postsynaptic NMDA receptors in the central nucleus of the amygdala in opioid dependence. Vitam. Horm 2010;82:145–66. [PubMed: 20472137]

Glass MJ, Vanyo L, Quimson L, Pickel VM. Ultrastructural relationship between NMDANR1 and mu-opioid receptor in the mouse central nucleus of the amygdala. Neurosci 2009;163:857–67.

Greger IH, Esteban JA. AMPA receptor biogenesis and trafficking. Curr. Opin. Neurobiol 2007;17:289–97. [PubMed: 17475474]

Hara Y, Pickel VM. Preferential relocation of the N-methyl-D-aspartate receptor NR1 subunit in nucleus accumbens neurons that contain dopamine D1 receptors in rats showing an apomorphine-induced sensorimotor gating deficit. Neurosci 2008;154:965–77.

He Y, Janssen WG, Morrison JH. Synaptic coexistence of AMPA and NMDA receptors in the rat hippocampus: a postembedding immunogold study. J. Neurosci. Res 1998;54:444–9. [PubMed: 9822155]

He Y, Janssen WG, Morrison JH. Differential synaptic distribution of the AMPA-GluR2 subunit on GABAergic and non-GABAergic neurons in the basolateral amygdala. Brain Res 1999;827:51–62. [PubMed: 10320693]

Hof, PR.; Young, EG.; Bloom, FE.; Belichenko, PV.; Celio, MR. Comparative cytoarchitectonic atlas of the C57BL/6 and 129/SV mouse brains. Elsevier, Elsevier; 2000.

Jaferi A, Pickel VM. Mu-opioid and corticotropin-releasing-factor receptors show largely postsynaptic co-expression,and separate presynaptic distributions, in the mouse central amygdala and bed nucleus of the stria terminalis. Neurosci 2009;159:526–39.

Kawasaki Y, Jin C, Suemaru K, Kawasaki H, Shibata K, Choshi T, Hibino S, Gomita Y, Araki H. Effect of glutamate receptor antagonists on place aversion induced by naloxone in single-dose morphine-treated rats. Br. J. Pharmacol 2005;145:751–7. [PubMed: 15880144]

Kishi T, Tsumori T, Yokota S, Yasui Y. Topographical projection from the hippocampal formation to the amygdala: a combined anterograde and retrograde tracing study in the rat. J. Comp. Neurol 2006;496:349–68. [PubMed: 16566004]

Klein G, Juni A, Arout CA, Waxman AR, Inturrisi CE, Kest B. Acute and chronic heroin dependence in mice: contribution of opioid and excitatory amino acid receptors. Eur. J. Pharmacol 2008;586:179–88. [PubMed: 18343363]

Knapska E, Radwanska K, Werka T, Kaczmarek L. Functional internal complexity of amygdala: focus on gene activity mapping after behavioral training and drugs of abuse. Physiol. Rev 2007;87:1113–73. [PubMed: 17928582]

Koob GF, Volkow ND. Neurocircuitry of addiction. Neuropsychopharmacol 2010;35:217–38.

Lang PJ, Davis M. Emotion, motivation, and the brain: reflex foundations in animal and human research. Prog. Brain Res 2006;156:3–29. [PubMed: 17015072]

Layer RT, Uretsky NJ, Wallace LJ. Effects of the AMPA/kainate receptor antagonist DNQX in the nucleus accumbens on drug-induced conditioned place preference. Brain Res 1993:617.

LeDoux JE. Emotion circuits in the brain. Ann. Rev. Neurosci 2000;23:155–184. [PubMed: 10845062]

Leranth, C.; Pickel, VM. Electron microscopic pre-embedding double immunostaining methods. In: Heimer, L.; Zaborszky, L., editors. Tract tracing methods 2, recent progress. Plenum; New York: 1989. p. 129-172.

Lerma J, Morales M, Ibarz JM, Somohano F. Rectification properties and Ca2+ permeability of glutamate receptor channels in hippocampal cells. Eur. J. Neurosci 1994;6:1080–8. [PubMed: 7524964]

Mansour A, Fox CA, Akil H, Watson SJ. Opioid-receptor mRNA expression in the rat CNS: anatomical and functional implications. Trends Neurosci 1995;18:22–29. [PubMed: 7535487]

Mansour A, Khachaturian H, Lewis ME, Akil H, Watson SJ. Anatomy of CNS opioid receptors. Trends Neurosci 1988;11:308–314. [PubMed: 2465635]

McDonald AJ. Cortical pathways to the mammalian amygdala. Prog. Neurobiol 1998;55:257–332. [PubMed: 9643556]

Mead AN, Morris HV, Dixon CI, Rulten SL, Mayne LV, Zamanillo D, Stephens DN. AMPA receptor GluR2, but not GluR1, subunit deletion impairs emotional response conditioning in mice. Behav. Neurosci 2006;120:241–8. [PubMed: 16719688]

Migues PV, Hardt O, Wu DC, Gamache K, Sacktor TC, Wang YT, Nader K. PKMzeta maintains memories by regulating GluR2-dependent AMPA receptor trafficking. Nature Neurosci 2010;13:630–4. [PubMed: 20383136]

Palmer CL, Cotton L, Henley JM. The molecular pharmacology and cell biology of alpha-amino-3-hydroxy-5-methyl-4-isoxazolepropionic acid receptors. Pharmacol. Rev 2005;57:253–77. [PubMed: 15914469]

Peters, A.; Palay, SL.; Webster, H. The fine structure of the nervous system. Oxford University Press, Oxford University Press; 1991.

Petralia RS, Wang YX, Mayat E, Wenthold RJ. Glutamate receptor subunit 2-selective antibody shows a differential distribution of calcium-impermeable AMPA receptors among populations of neurons. J. Comp. Neurol 1997;385:456–76. [PubMed: 9300771]

Petralia RS, Wenthold RJ. Light and electron immunocytochemical localization of AMPA-selective glutamate receptors in the rat brain. J. Comp. Neurol 1992;318:329–54. [PubMed: 1374769]

Pitkanen A, Savander V, LeDoux JE. Organization of intra-amygdaloid circuitries in the rat: an emerging framework for understanding functions of the amygdala. Trends in Neurosci 1997;20:517–23.

Poulin JF, Chevalier B, Laforest S, Drolet G. Enkephalinergic afferents of the centromedial amygdala in the rat. J. Comp. Neurol 2006;496:859–76. [PubMed: 16628615]

Rasmussen K, Vandergriff J. The selective iGluR1-4(AMPA) antagonist LY300168 attenuates morphine-withdrawal-induced activation of locus coeruleus neurons and behavioural signs of morphine withdrawal. Neuropharmacol 2003;44:88–92.

Sacktor TC. PKMzeta, LTP maintenance, and the dynamic molecular biology of memory storage. Prog. Brain Res 2008;169:27–40. [PubMed: 18394466]

Sato K, Kiyama H, Tohyama M. The differential expression patterns of messenger RNAs encoding non-N-methyl-D-aspartate glutamate receptor subunits (GluR1-4) in the rat brain. Neurosci 1993;52:515–39.

Sepehrizadeh Z, Bahrololoumi Shapourabadi M, Ahmadi S, Hashemi Bozchlou S, Zarrindast MR, Sahebgharani M. Decreased AMPA GluR2, but not GluR3, mRNA expression in rat amygdala and dorsal hippocampus following morphine-induced behavioural sensitization. Clini. Exp. Pharmacol. Physiol 2008;35:1321–30.

Shindou T, Watanabe S, Yamamoto K, Nakanishi H. NMDA receptor-dependent formation of long-term potentiation in the rat medial amygdala neuron in an in vitro slice preparation. Brain Res. Bulletin 1993;31:667–72.

Spruston N, Jonas P, Sakmann B. Dendritic glutamate receptor channels in rat hippocampal CA3 and CA1 pyramidal neurons. J. Physiol 1995;482:325–52. [PubMed: 7536248]

Taylor JR, Punch LR, Elsworth JD. A comparison of the effects of clonidine and CNQX infusion into the locus coeruleus and the amygdala on naloxone-precipitated opiate withdrawal in the rat. Psychopharmacol 1998;138:133–142.

Turner BH, Herkenham M. Thalamoamygdaloid projections in the rat: a test of the amygdala's role in sensory processing. J. Comp. Neurol 1991;313:295–325. [PubMed: 1765584]

Tzschentke TM, Schmidt WJ. Interactions of MK-801 and GYKI 52466 with morphine and amphetamine in place preference conditioning and behavioural sensitization. Behav. Brain Res 1997;84:99–107. [PubMed: 9079776]

Van den Oever MC, Goriounova NA, Li KW, Van der Schors RC, Binnekade R, Schoffelmeer AN, Mansvelder HD, Smit AB, Spijker S, De Vries TJ. Prefrontal cortex AMPA receptor plasticity is crucial for cue-induced relapse to heroin-seeking. Nature Neurosci 2008;11:1053–8. [PubMed: 19160503]

Wang H, Cuzon VC, Pickel VM. Postnatal development of mu-opioid receptors in the rat caudate-putamen nucleus parallels asymmetric synapse formation. Neurosci 2003;118:695–708.

Watanabe T, Nakagawa T, Yamamoto R, Maeda A, Minami M, Satoh M. Involvement of glutamate receptors within the central nucleus of the amygdala in naloxone-precipitated withdrawal-induced conditioned place aversion in rats. Jpn. J. Pharmacol 2002;88:399–406. [PubMed: 12046982]

Zhong W, Dong Z, Tian M, Cao J, Xu T, Xu L, Luo J. Opiate withdrawal induces dynamic expressions of AMPA receptors and its regulatory molecule CaMKIIalpha in hippocampal synapses. Life Sci 2006;79:861–9. [PubMed: 16616767]

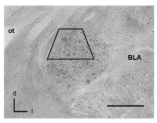

Figure 1. GluR2 expressing neurons are present in the CeA as shown by light microscopy
Immunoperoxidase labeling for GluR2 is present in cell bodies throughout the CeA. The region bounded by the trapezoid represents the area sampled by electron microscopy. BLA: basolateral nucleus: d=dorsal; l=lateral; ot=optic tract. Scale Bar= 0.5 mm.

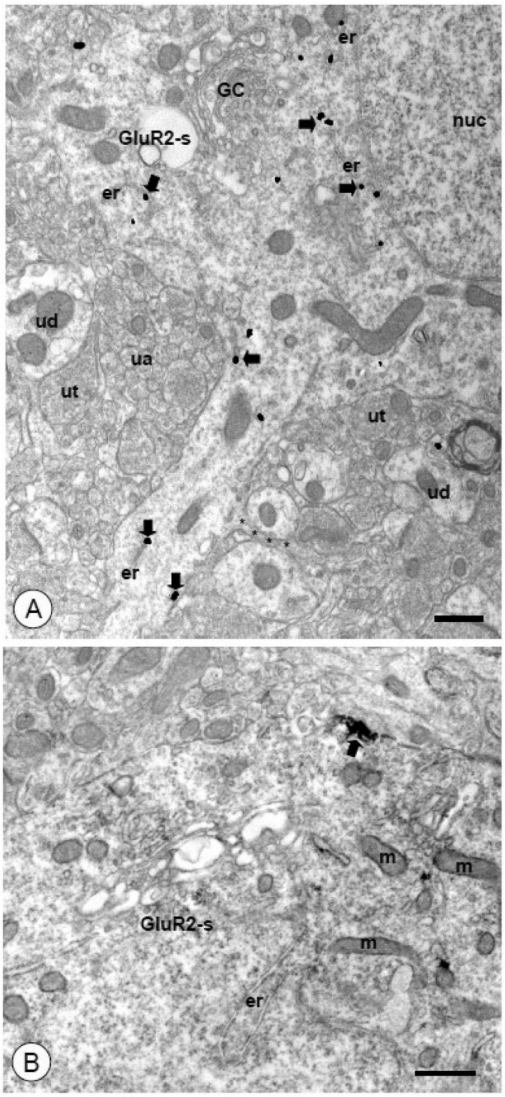

Figure 2. Somata of CeA neurons express intracellular and surface GluR2

(A). A somatodendritic (GluR2-s) profile is present in the neuropil populated by unlabeled profiles of dendrites (ud), axons (ua), and axon terminals (ut). A nucleus (nuc), as well as Golgi Complexes (GC) and endoplasmic reticula (er) can be seen within the soma. Immunogold-silver particles for GluR2 (arrows) are present near vesicular organelles in the perinuclear cytoplasm. Particles are also found in a process emanating from the cell body. A small unlabeled appendage (asterisks) can be seen extending from the larger dendritic structure. **(B)**. A soma (GluR2-s) containing endomembranous organelles (er) and mitochondria (m) shows discrete immuoperoxidase labeling for GluR2 (arrow). A dense punctate aggregation of immunoperoxidase reaction product is present beneath the plasma membrane.

Scale Bars= 0.5 μm.

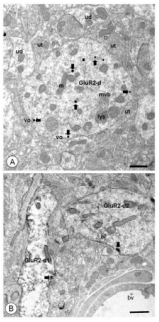

Figure 3. Large and medium-size dendritic processes of CeA neurons express intracellular and surface GluR2

(A). A large GluR2 labeled proximal dendritic profile (GluR2-d) is present in the neuropil along with unlabeled dendrites (ud) and axon terminals (ut). The GluR2 labeled dendrite contains small vesicular organelles (vo), mitochondria (m), lysosomes (lys), and multivesicular bodies (mvb). Intracellular immunogold-silver particles for GluR2 (arrows) are present throughout the profile. This dendritic profile is contacted by unlabeled axon terminals (ut) that do not form obvious synaptic specializations. **(B)**. Dendritic profiles (GluR2-d1 and GluR1-d2) adjacent to a blood vessel (bv) show discrete immuoperoxidase reaction product for GluR2 (arrows) in intracellular and surface compartments. Discrete patches of GluR2 immunoreactivity are present near the plasmalemma of a longitudinally sectioned medium-size dendritic profile (GluR2-d1). A dense aggregate of immunoperoxidase labeling is present beneath the plasma membrane of a large coronally sectioned dendritic profile (GluR2-d2). Scale Bars= 0.5 μm.

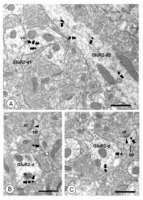

Figure 4. Intermediate-size and small dendrites with spiny appendages express intracellular and surface GluR2

(A). Two dendritic profiles (GluR2-d1 and GluR1-d2) oriented in different planes of section express GluR2 labeling. A small dendritic process (GluR2-d1) with an apparent spine neck (asterisks) shows a cluster of immunogold particles for GluR2 (arrows) near a vesicular organelle (vo) just beneath the plasma membrane. Labeling for GluR2 is also present in a longitudinally sectioned dendritic profile (GluR2-d2). In this structure, immunogold particles (arrows) are affiliated with intracellular organelles, as well as non-synaptic areas of the plasma membrane. **(B).** A small dendritic profile (GluR2-d) with a spiny appendage (asterisks) expresses GluR2. Immunogold particles (arrows) are associated with the plasmalemma in the dendritic shaft, and a single gold particle is present in the spine neck (arrow). An asymmetric synaptic junction (arrowhead) is formed between an unlabeled axon terminal (ut) and the spine head (sp), which is devoid of GluR2 labeling. **(C)**. The shaft of a small dendritic profile shows GluR2 labeling (arrows) on the plasma membrane distal from a spine neck (asterisks). An adjacent spine head (sp) contains a single gold particle beneath the postsynaptic density (arrowhead) of an asymmetric-type junction. Scale Bars= 0.5 μm.

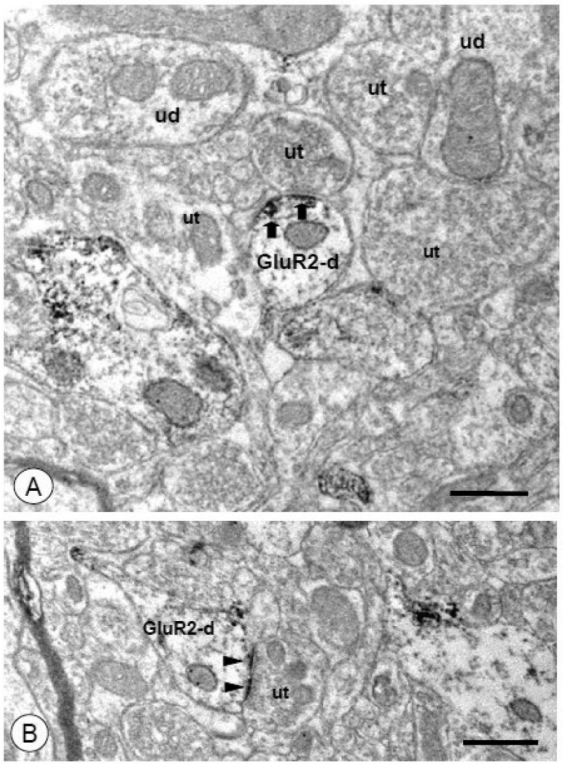

Figure 5. Small-size dendritic profiles of CeA neurons express plasmalemmal and synaptic GluR2

(A). A small GluR2 labeled dendritic profile (GluR2-d) is contacted by a small unlabeled axon terminal (ut). Aggregates of immunoperoxidase for GluR2 (arrows) are present near the plasma membrane adjacent to the apposing axon terminal. Unlabeled dendritic (ud) and axonal (ut) profiles are present in the surrounding neuropil. **(B).** An asymmetric synaptic junction is formed between an unlabeled axon terminal (ut) and a GluR2 expressing small dendritic profile (GluR2-d). The perforated postsynaptic density in this dendrite shows immunoperoxidase reaction product for GluR2 (arrowheads). Scale Bars= 0.5 μm.

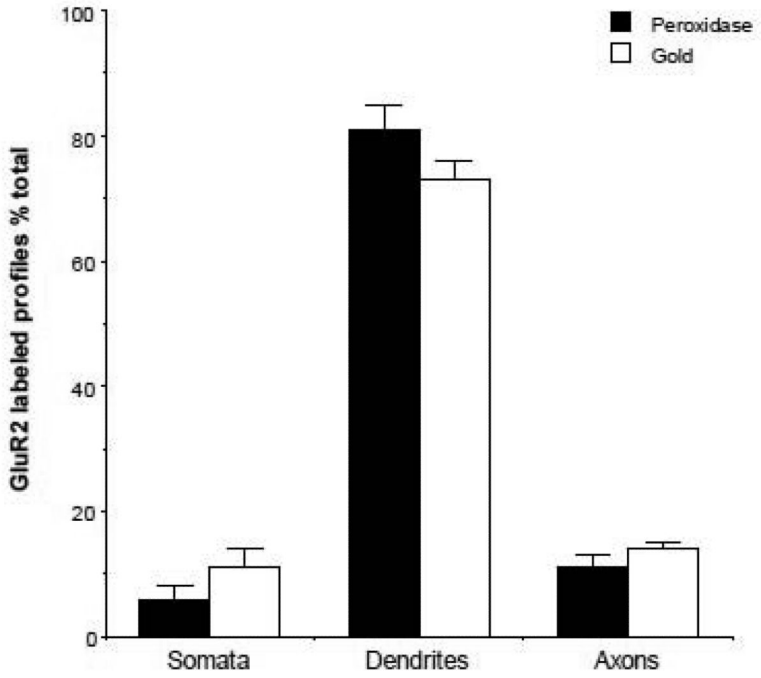

Figure 6. GluR2 is highly expressed in dendrites of CeA neurons

Histogram showing the relative distribution of immunoperoxidase (Peroxidase) and immunogold (Gold) GluR2 labeling in distinct compartments (somata, dendrites, axons) of CeA neurons. When calculated as a percentage of all labeled profiles, GluR2 is mainly found in dendrites. This pattern is similar when GluR2 is labeled with peroxidase or gold markers.

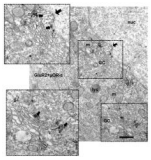

Figure 7. Somata of CeA neurons express both GluR2 and μOR

A neuronal soma (GluR2+μOR-s) with diverse intracellular organelles, including Golgi Complexes (GC), lysosomes (lys), and mitochondria (m), contains GluR2 and μOR labeling. At the higher magnification shown in the insets, immunoperoxidase reaction product for GluR2 (filled arrows) can be seen near GCs, one of which **(top inset)** is in the perinuclear cytoplasm close to a nuclear (nuc) invagination (notched arrow). Immunogold particles for μOR (open arrows) are also present in the same structures, including closely apposed areas of the same organelle **(top and bottom insets)**. Scale Bar= 0.5 μm

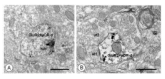

Figure 8. Small dendritic processes of CeA neurons express both GluR2 and μOR

(A). A small dendritic profile (GluR2+μOR-d) shows immunoperoxidase labeling for GluR2 (arrow) and immunogold labeling for μOR (open arrows). A dense aggregation of immunoperoxidase reaction product for GluR2 is seen near the plasma membrane and an associated tubulovesicular organelle (tub). Immunogold particles for μOR are also present on the extrasynaptic plasmalemma. **(B).** A small dual labeled dendritic profile (GluR2+μOR-d) is contacted by unlabeled axon terminals (ut1, ut2). A postsynaptic specialization, which also appears to express immunoperoxidase reaction product (arrows), is formed by one of these terminals (ut1). Immunogold μOR labeling (open arrows) is present on the nearby extrasynaptic membrane as well as intracellularly. Scale Bars= 0.5 μm

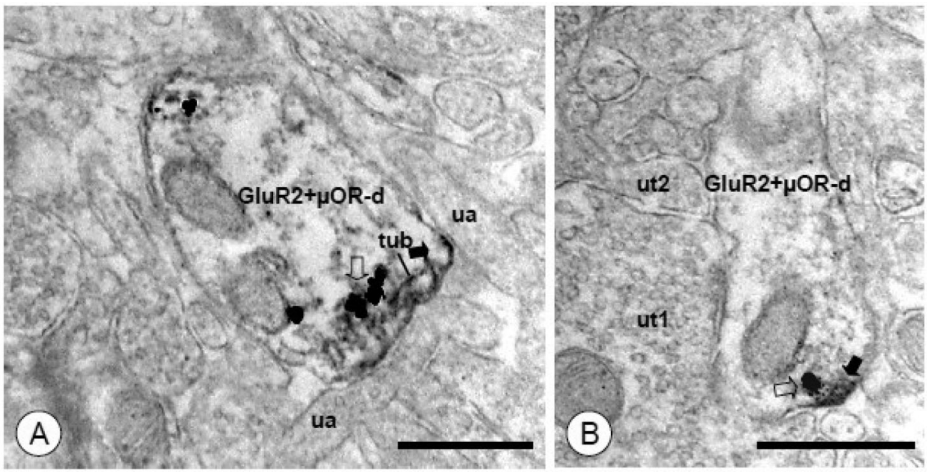

Figure 9. GluR2 and μOR labeling are found in closely apposed subcellular structures in dendritic profiles of CeA neurons

(A). A dual labeled dendritic profile (GluR2+μOR-d) is contacted by unlabeled axons (ua). Immunoperoxidase labeling for GluR2 (filled arrow) is present near the surface membrane, as well as an adjacent tubulovesicular organelle (tub). A cluster of immunogold particles for μOR (open arrow) is present on an adjacent membrane. **(B).** A dendritic profile shows discrete immunoperoxidase reaction product for GluR2 (arrow) near the plasma membrane. A single immunogold-silver particle for μOR (open arrow) is present in an adjoining membrane. Unlabeled axon terminals (ut1, ut2) are adjacent to this dendrite. Scale Bars= 0.5 μm

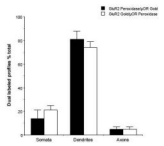

Figure 10. Dual GluR2 and μOR labeling is mainly present in dendrites of CeA neurons

Histogram showing the relative distribution of GluR2 and μOR co-labeling in distinct compartments (somata, dendrites, axons) of CeA neurons. When calculated as a percentage of all dual labeled profiles, dendrites and somata are the most common neuronal structures expressing labeling for both proteins. This pattern is similar when GluR2 is labeled with immunoperoxidase (GluR2 Peroxidase) and μOR with immunogold (μOR Gold) and when the markers are reversed (GluR2 Gold/μOR Peroxidase).

Table 1

Number of labeled profiles in the CeA obtained from tissue processed for single gold or peroxidase labeling of GluR2

	Somata	Dendrites	Axons
Gold	35	323	72
Peroxidase	41	749	96

Table 2

Number of single or co-labeled profiles in CeA of tissue processed for dual GluR2 and μOR labeling.

	GluR2 Peroxidase/μOR Gold	1% (2)	84% (268)	15% (48)
Single GluR2	GluR2 Gold/μOR Peroxidase	4% (11)	72% (204)	24%(69)
	GluR2 Peroxidase/μOR Gold	7% (13)	62% (121)	31% (60)
Single μOR	GluR2 Gold/μOR Peroxidase	2% (13)	75% (456)	23% (141)
	Dual GluR2 Peroxidase/μOR Gold	15% (9)	80% (47)	5% (3)
GluR2+μOR	Dual GluR2 Gold/μOR Peroxidase	19% (28)	76% (113)	5% (8)